

# Mechanism of the quasi-elastic scattering based on the dinuclear system concept

Zehong Liao, Yu Yang, Zepeng Gao, Jun Su, and Long Zhu\*

Sino-French Institute of Nuclear Engineering and Technology, Sun Yat-sen University, Zhuhai 519082, China

(Dated: September 5, 2025)

A unified description of full reaction channels in low-energy heavy-ion collisions is a great challenge. Although, the theoretical models based on the dinuclear system (DNS) concept have been successfully employed in multinucleon transfer (MNT) reactions, the underestimation of the quasi-elastic (QE) channel results in unreliable description of few nucleon transfer, especially for the light reaction systems. In this work, the DNS-sysu model is improved by introducing the impact-parameter-dependent transition probabilities for a unified description of few nucleon and many nucleon transfer in MNT reactions. Extensive experimental data—including reactions such as  $^{40}\text{Ca}$ ,  $^{58,64}\text{Ni}$ ,  $^{136}\text{Xe}$ , and  $^{208}\text{Pb} + ^{208}\text{Pb}$  were compared with the model predictions. The calculated isotopic distributions, mass distributions, and charge distributions show good agreement with experimental measurements. The improved DNS-sysu model enables reasonable characterization and description of the QE/grazing collisions, notably resolving long-standing underestimation in the QE channel.

*Introduction.* The complexity of multinucleon transfer (MNT) reactions originates from the coexistence of multiple overlapping processes, most notably quasi-elastic (QE) scattering, deep-inelastic (DI) scattering, and quasi-fission (QF)[1]. Experimental observables such as the TKE-mass distribution in conjunction with the TKEL distribution of the reaction products provide Importance probes of these channels and reveal their intricate interplay [2–10]. Various phenomenological and microscopic approaches have been developed to describe these processes, including the Grazing model [11, 12], the dinuclear system (DNS) model [13–18], the Langevin-type transport model [19, 20], the Coupled Master and Langevin equations [21, 22], the quantum molecular dynamics simulation [23–25], the time-dependent mean-field theory [26–29], and beyond mean-field approaches [30, 31].

Among these, the DNS model stands out for its intuitive picture of two touching nuclei forming a interacting dinuclear configuration, a concept first proposed by Volkov [32]. The treatment of the internuclear distance as a frozen degree of freedom is a reasonable approximation in MNT reactions, where the configuration is sufficiently long-lived to permit extensive nucleon exchange. Owing to this physical picture, the DNS model has been successfully applied to reproduce a variety of experimental observables in MNT reactions [33–36], demonstrating remarkable predictive power. Nevertheless, the applicability of the DNS picture becomes questionable in the regime of grazing collisions/QE [17, 37]. In such QE events, only a few nucleons are exchanged, and the interacting nuclei remain relatively far apart with a short-lived contact time. Under these conditions, the assumption of a frozen internuclear distance and a well-formed dinuclear configuration no longer holds, leading to poor performance of the DNS model in describing the QE channel.

The primary objective of this work is to develop such a theoretical model capable of consistently characterizing the QE scattering, DI scattering, and QF processes. We aim to improve the DNS model by introducing a nucleon exchange distance that incorporates relaxation behavior, thereby providing a more accurate and comprehensive description of multinucleon transfer reactions in heavy-ion collisions.

*Theoretical framework.* The DNS-sysu model is based on the master equation that simulates the evolution of the probability distribution of collective degrees of freedom in non-equilibrium processes. The version of model developed in this work is based on the same foundational framework as that of Zhu *et al.* [38] and can be regarded as an extension and further development of the approach. The proposed methodology comprises several key components:

- i) The multi-dimensional potential energy surface (PES) that characterize the full reaction landscape, including the dynamical deformation  $\beta_2$ , proton number  $Z_1$ , and neutron number  $N_1$ , providing the driving forces for the evolution of the system.
- ii) A three-dimensional master equation that governs the time evolution of probability distributions associated with various nuclear reaction channels, allowing for a quantitative description of the non-equilibrium dynamics in terms of transition rates between different states.
- iii) The transfer rates that quantify the likelihood of exchanging nucleons between the interacting nuclei depend not only on the system size and the excitation energy during the reaction [39], but also on the collision parameters.
- iv) The deflection function method [40] provides the model with a reaction time that depends on the deflection parameter.

The PES describes the potential energy values that correspond to all possible configurations of a reaction

\* Contact author: zhulong@mail.sysu.edu.cn

system. By analyzing its geometric features (including minima, saddle points, and gradients), one can gain intuitive understanding of how the system evolves between different states. The PES in the DNS-sysu model can be expressed as:

$$U(Z_1, N_1, \beta_2, J, R_{\text{cont}}) = \Delta(Z_1, N_1) + \Delta(Z_2, N_2) + V_{\text{cont}}(Z_1, N_1, \beta_2, J, R_{\text{cont}}) + \frac{1}{2}C_1(\delta\beta_2^1)^2 + \frac{1}{2}C_2(\delta\beta_2^2)^2. \quad (1)$$

Here,  $\Delta(Z_i, N_i)$  ( $i=1,2$ ) is the mass excess of the  $i$ th fragment [41]. The last two terms are dynamical deformation energies of the projectile-like fragment (PLF) and target-like fragment (TLF). We restricted the consideration of only one dynamic deformation parameter  $\beta_2$  instead of two independent deformation  $\beta_2^1$  and  $\beta_2^2$  [42]. The dynamical deformation for each fragment can be calculated by  $C_1\delta\beta_2^1 = C_2\delta\beta_2^2$  and  $\delta\beta_2^1 + \delta\beta_2^2 = 2\beta_2$ . The quadrupole deformation parameters of PLF and TLF are given by  $\beta_2^1 = \beta_2^p + \delta\beta_2^1$  and  $\beta_2^2 = \beta_2^t + \delta\beta_2^2$ , respectively.  $\beta_2^p$  and  $\beta_2^t$  are static quadrupole deformation parameters of the projectile and target, respectively.  $C_{1,2}$  are the LDM stiffness parameters of the fragments [43]. For the  $\beta_2$ , we take the range of -0.5 to 0.5. The evolution step length is 0.01. The range of  $Z_1$  ( $N_1$ ) is from 1 to  $Z_{\text{tot}}$  ( $N_{\text{tot}}$ ), with a step size of 1.  $R_{\text{cont}}$  is the position where the nucleon transfer process takes place. In the present work, this quantity has been modified to account for its dependence on the collision parameter, exhibiting a relaxation behavior that will be discussed in detail later. The effective nucleus-nucleus interaction potential consists of the long-range Coulomb repulsive potential, the attractive short-range nuclear potential, and the centrifugal potential:

$$V(Z_1, N_1, \beta_2, J, r) = V_N(Z_1, N_1, \beta_2, r) + V_C(Z_1, N_1, \beta_2, r) + \frac{J(J+1)\hbar^2}{2\zeta_{\text{rel}}}. \quad (2)$$

Here,  $\zeta_{\text{rel}}$  is the moment of inertia for the relative motion of the DNS. More detailed description of Coulomb potential  $V_C$  and nuclear potential  $V_N$  can be seen in Refs. [44–46].

The MNT reactions involve multiple reaction channels, including QE scattering, DI scattering, and QF processes, which represent distinct dynamical evolution pathways. The intensity of nucleon exchange between the nuclei is expected to correlate with the distance between colliding partners. For the QE scattering/grazing collisions, the nuclear potential exerts a relatively weak attraction on the projectile, causing its trajectory to closely follow that of Rutherford scattering. As a result, the two nuclei remain at relatively large distances throughout the interaction and the relaxation time is rather short. And the distance of closest approach  $R_{\text{closest}}$  can be obtained

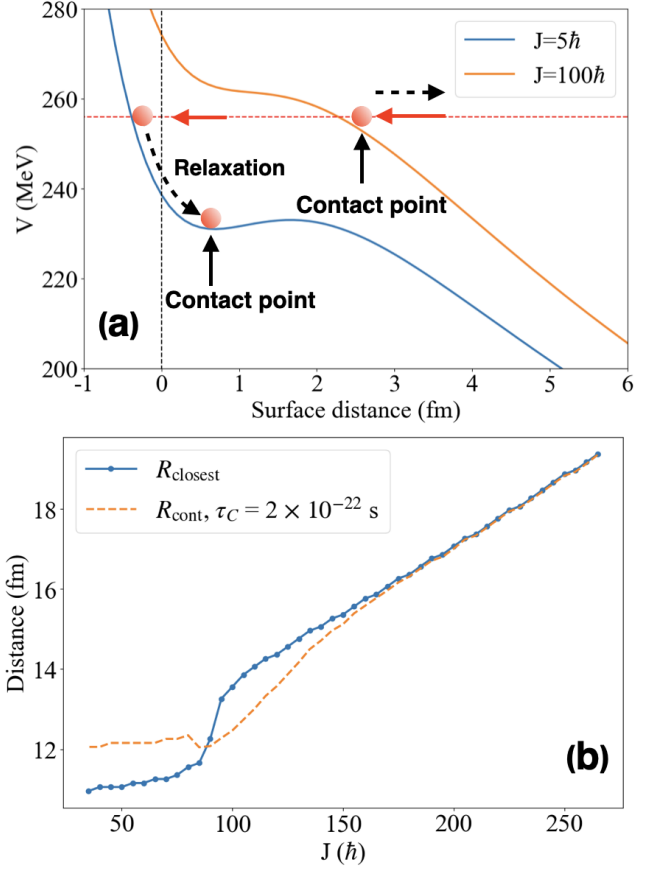


FIG. 1. Top panel: Contact points for the  $^{58}\text{Ni} + ^{208}\text{Pb}$  system at  $J = 5 \hbar$  and  $100 \hbar$ . The horizontal dashed line represents the incident energy, while the vertical dashed line indicates the sum of the radii of the two nuclei. Bottom panel: The contact position as a function of the entrance angular momentum.

by equilibrating the incident energy and the interaction potential  $V(Z_{\text{pro}}, N_{\text{pro}}, \beta_2 = 0, J, r)$ . As the reaction progresses toward more violent collisions, usually corresponding to smaller impact parameters, the internuclear separation decreases significantly. Due to the Pauli exclusion principle, the internuclear distance cannot become too small. Instead, nucleon exchange typically occurs with a long relaxation time when the system resides at a relatively flat region of the potential energy surface, such as near the bottom of the potential pocket ( $R_{\text{bottom}}$ ). For systems without a potential pocket, this value  $R_{\text{bottom}}$  is taken at a surface separation of approximately 0.7 fm. Therefore, in this work, the contact distance between the nuclei is represented phenomenologically by introducing a relaxation behavior:

$$R_{\text{cont}} = R_{\text{closest}}f(t) + R_{\text{bottom}}[1 - f(t)]. \quad (3)$$

Here  $t$  is the interaction time at each angular momentum, obtained through the deflection function [40].  $f(t) = \exp(-t/\tau_C)$  is a smoothing function with characteristic time  $\tau_C = 2 \times 10^{-22}$  s. The relaxation time can be deter-

mined from the analysis of experimental data.

In the case of QE scattering, such as when the relative angular momentum is around  $100 \hbar$  as shown in the Fig. 1(a), the extremely short interaction time ( $t \leq 10^{-22}$  s) prevents any significant relaxation. After reaching the point of closest approach, the nuclei are immediately scattered apart. However, as the collision becomes more violent, strong friction forces and large nuclear viscosity in the entrance channel drive the system toward relaxation, gradually settling into the flatter region of the adiabatic potential where nucleon exchange occurs. These two distinct dynamical regimes are schematically illustrated in Fig. 1 (a). In Fig. 1(b), the blue line represents the closest approach distance between the nuclei as a function of angular momentum, while the red dashed line includes the effect of relaxation behavior. It can be observed that in the region of large angular momentum (the QE scattering case), the difference between the two curves is negligible. However, at low angular momentum, the relaxed contact distance tends to stabilize around a specific value.

The master equation (ME) describes the evolution of the probability distribution of states of a continuous-time

Markov process [47]. The general form of the ME can be written as:

$$\frac{\partial P(\mathbf{S}, t)}{\partial t} = \sum_{\mathbf{S}' \neq \mathbf{S}} W(\mathbf{S}', \mathbf{S}) P(\mathbf{S}', t) - W(\mathbf{S}, \mathbf{S}') P(\mathbf{S}, t). \quad (4)$$

$P(\mathbf{S}, t)$  denotes the occupation probability of state  $\mathbf{S}$ . The quantity  $W$  is transition probability per time unit or transition rate in the following sense:  $W(\mathbf{S}', \mathbf{S}) P(\mathbf{S}', t)$  is the probability transferred from state  $\mathbf{S}'$  to the state  $\mathbf{S}$  per unit of time.

In the DNS-sysu model, the number of proton  $Z_1$ , the number of neutron  $N_1$ , and the dynamical deformation  $\beta_2$  degree of freedom for describing the macroscopic observables of PLF. Hence,  $\mathbf{S} = (Z_1, N_1, \beta_2)$ . In this model, each time step permits only a single transition to an adjacent macroscopic state, corresponding to a one-unit change in either  $Z_1$  or  $N_1$ , with the spatial scale of the macroscopic states precisely matching the potential energy surface grid defined in the previous section. Therefore, the joint probability of fragments  $P$  evolving with different macroscopic degrees of freedom can be solved numerically as follows:

$$\begin{aligned} \frac{\partial P(\beta_2, Z_1, N_1, t)}{\partial t} = & W(\beta_2 - \Delta\beta_2, \beta_2) P(\beta_2 - \Delta\beta_2, Z_1, N_1, t) + W(\beta_2 + \Delta\beta_2, \beta_2) P(\beta_2 + \Delta\beta_2, Z_1, N_1, t) \\ & + W(Z_1 - \Delta Z, Z_1) P(\beta_2, Z_1 - \Delta Z, N_1, t) + W(Z_1 + \Delta Z, Z_1) P(\beta_2, Z_1 + \Delta Z, N_1, t) \\ & + W(N_1 - \Delta N, N_1) P(\beta_2, Z_1, N_1 - \Delta N, t) + W(N_1 + \Delta N, N_1) P(\beta_2, Z_1, N_1 + \Delta N, t) \\ & - [W(\beta_2, \beta_2 + \Delta\beta_2) + W(\beta_2, \beta_2 - \Delta\beta_2)] P(\beta_2, Z_1, N_1, t) \\ & - [W(Z_1, Z_1 + \Delta Z) + W(Z_1, Z_1 - \Delta Z)] P(\beta_2, Z_1, N_1, t) \\ & - [W(N_1, N_1 + \Delta N) + W(N_1, N_1 - \Delta N)] P(\beta_2, Z_1, N_1, t). \end{aligned} \quad (5)$$

Here,  $W(Z_1 - \Delta Z, Z_1)$  represents the macroscopic transition rate from the channel  $(Z_1 - \Delta Z, N_1, \beta_2)$  to  $(Z_1, N_1, \beta_2)$ , and the other macroscopic transition rates are similar. A single transition is restricted to interactions between adjacent macroscopic states; that is, transitions occur with  $\Delta Z = 1$ ,  $\Delta N = 1$ , and  $\Delta\beta_2 = 0.01$ .

The transfer rate  $W$  serves as a critical bridge between microscopic nucleon exchange mechanisms and macroscopic observables. For nuclei in contact the macroscopic transition rate can be treated by [20, 48]:

$$W(\mathbf{S}', \mathbf{S}) \propto \lambda_0 \exp\left(\frac{U(\mathbf{S}') - U(\mathbf{S})}{2T}\right). \quad (6)$$

Although,  $\lambda_0$  ( $\approx 10^{22} \text{s}^{-1}$ ) serves as the nucleon transfer rate in the model, its derivation from first principles, particularly its coupling to dissipation dynamics and potential energy gradients, has yet to be rigorously established. As usual, it can be qualitatively assumed that it is related to the size of the system and the temperature

[48, 49]. In this study, we adopt the nucleon transfer rate identical to that ( $5 \times A_{\text{tot}}^2 \times (T/\text{MeV}) \times 10^{16}$ ) reported in Ref. [39], ensuring consistency with established theoretical benchmarks for comparative analysis.

The term  $\exp(\frac{U(\mathbf{S}') - U(\mathbf{S})}{2T})$  governs the thermally driven transitions between macroscopic states  $\mathbf{S}'$  and  $\mathbf{S}$  in the master equation. Here,  $U(\mathbf{S})$  denotes the potential energy of the collective coordinates (*e.g.*, fragment( $Z_1, N_1$ ), dynamical deformation  $\beta_2$ ), while  $T$  represents the local nuclear temperature  $\sqrt{E^*}/\alpha$ ,  $E^*$  is the excitation energy,  $\alpha = A_{\text{tot}}/12 \text{ MeV}^{-1}$  is the level density parameter.

For separated nuclei, nucleon exchange/transfer could still take place depending on the extension of the tails of the single particle wavefunctions. This happens mainly through temporary connections (necks) between the nuclei, which is important for grazing collisions. Therefore, the transition rate  $W$  can be further written as the fol-

lowing expression [50, 51]:

$$W(\mathbf{S}', \mathbf{S}) = \lambda_0 \exp\left(\frac{U(\mathbf{S}') - U(\mathbf{S})}{2T}\right) P_{\text{tr}}(R_{\text{cont}}, \mathbf{S} \rightarrow \mathbf{S} \pm \Delta \mathbf{S}). \quad (7)$$

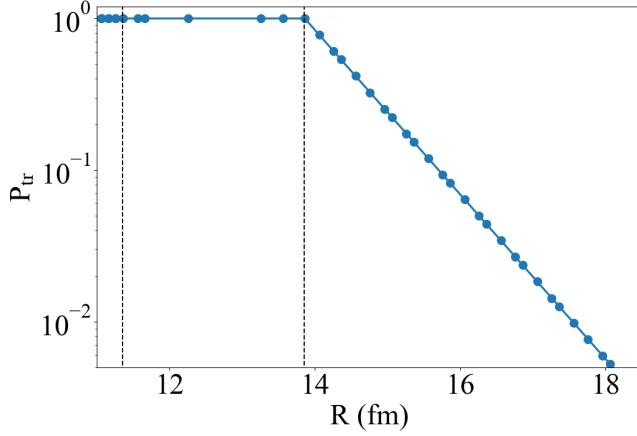


FIG. 2. The nucleon transfer probability as a function of the center distance in the reaction  $^{58}\text{Ni} + ^{208}\text{Pb}$  at  $E_{\text{c.m.}} = 256$  MeV.

Here,  $P_{\text{tr}}(R_{\text{cont}}, \mathbf{S} \rightarrow \mathbf{S} \pm \Delta \mathbf{S})$  is the probability of macroscopic degrees of freedom  $\mathbf{S}$  depends on the distance between the nuclear surfaces. The semiclassical approximation  $\exp(-2k[R - R_{\text{tr}}])$  is used for calculating  $P_{\text{tr}}$ .  $R_{\text{tr}} = R_{\text{pro}} + R_{\text{tar}} + 2.5$  fm. For the neutron,  $k = \sqrt{M(-\epsilon_F)/2\hbar^2} + \sqrt{M(-\epsilon'_F)/2\hbar^2}$ . For the proton,  $k = \sqrt{M(-\epsilon_F + Z_T e^2/R_T)/2\hbar^2} + \sqrt{M(-\epsilon'_F + Z_P e^2/R_P)/2\hbar^2}$ .  $M$  means the nucleon mass and  $\epsilon_F$  ( $\epsilon'_F$ ) denotes the nucleon separation energy of projectile (target). Figure 2 shows the nucleon transfer probability as a function of the internuclear separation  $R$ . Each data point corresponds to a simulation performed at the indicated collision angular momentum. The left vertical dashed line denotes the sum of the radii of the two nuclei, while the right one marks a surface separation of 2.5 fm. This probability goes exponentially to zero at  $R \rightarrow \infty$  and it is equal to unity when  $R$  is smaller than  $R_{\text{tr}}$ .

**Results and discussions.** Figure 3 shows the comparison of calculated charge distributions with the experimental data [52] for the MNT reaction  $^{58}\text{Ni} + ^{208}\text{Pb}$  at  $E_{\text{c.m.}} = 256$  MeV. The code GEMINI++ [53] is used to treat the de-excitation process of primary fragments.

Fig. 3 illustrates the significant improvement achieved by the DNS-sysu model with the QE channel in reproducing the experimental transfer cross sections, particularly for few-nucleon transfer processes. Note that experimental detection conditions are applied as constraints in the calculations. Specifically, we implement an angular momentum cutoff to select computational results that fall within the experimentally observable range. The DNS-sysu result without the QE channel clearly demonstrates

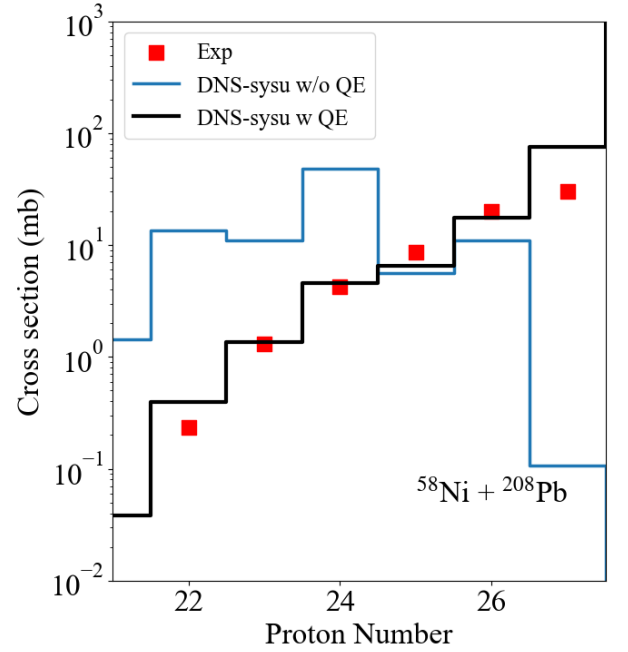


FIG. 3. Total cross sections for pure proton stripping channels in the reaction  $^{58}\text{Ni} + ^{208}\text{Pb}$  at  $E_{\text{c.m.}} = 256$  MeV. The blue line represents the DNS-sysu result without the QE channel. The black solid line represents the result with the QE channel.

its failure to describe and significant underestimation of the experimental data for one to two-proton transfer reactions. As discussed previously, this deficiency stems from the model's inherent limitation in accounting for long-range nucleon transfer probabilities. In contrast, the improved model shows excellent agreement with the few-nucleon transfer cross sections, successfully reproducing both the absolute values and the slope of the cross-section decrease as a function of transferred nucleon number.

In order to further test the improved DNS-sysu model, in Fig. 4, we present a systematic comparison of isotopic distributions between experimental data and calculations for four representative reaction systems: beams  $^{40}\text{Ca}$  and  $^{58}\text{Ni}$  incident on a  $^{208}\text{Pb}$  target at center-of-mass energies of  $E_{\text{c.m.}} = 197, 209$ , and  $256$  MeV [52, 54, 55], respectively. The calculations show excellent agreement with experimental data for the (0p) channel, accurately reproducing neutron pick-up cross sections. However, minor deviations emerge in the (-1p) channel, where the model slightly overestimates neutron pick-up cross sections while modestly underestimating neutron stripping values. These discrepancies become progressively more pronounced in the (-2p), (-3p), and (-4p) channels, demonstrating a systematic trend where the difference between theory and experiment grows with increasing number of protons removed from the projectile.

Moreover, the most significant difference between the original model and the improved one lies in the results for (0p) and (-1p) transfer. It is evident that the improved DNS-sysu model with consideration of angular momen-

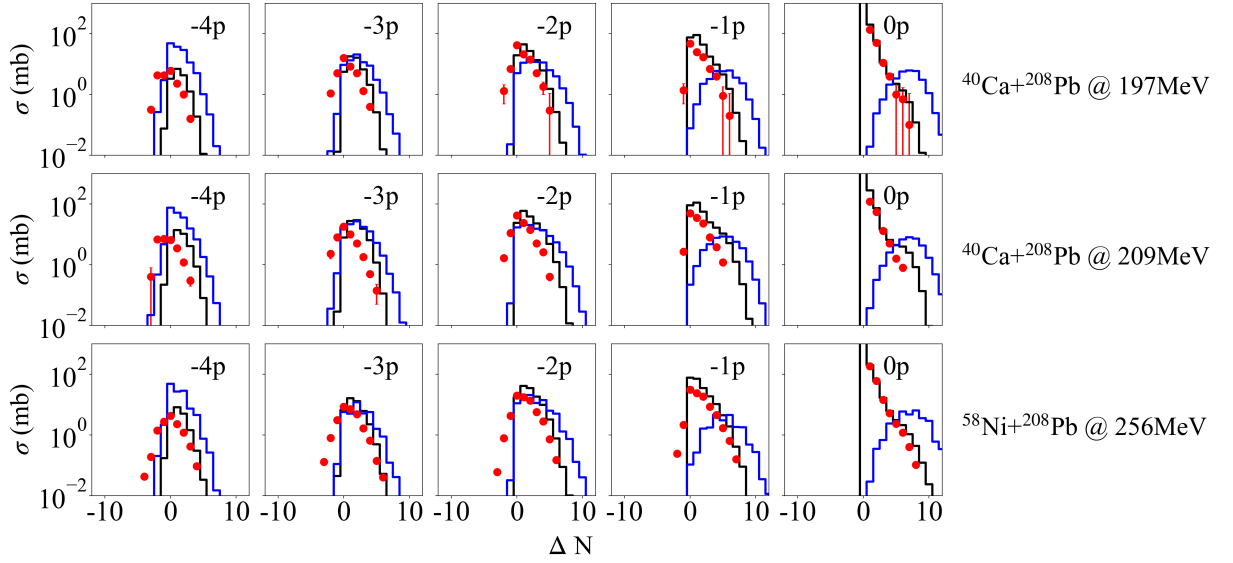


FIG. 4. Experimental cross sections for  $^{40}\text{Ca} + ^{208}\text{Pb}$  (the first and second row) and  $^{58}\text{Ni} + ^{208}\text{Pb}$  (the third row), at energies  $E_{\text{c.m.}} = 197, 209$ , and  $256$  MeV, respectively. The black and blue solid lines denote the calculated results with the improved and the origin DNS model, respectively.

tum dependent transition probability strongly improve the description of QE/grazing collisions.

In addition to comparing isotopic cross sections that directly reflect nucleon transfer patterns, we also systematically examine the distributions of reaction products that provide more intuitive characterization of collective behavior in MNT processes where massive nucleon redistribution occurs. The comparison of the available experimental data on mass or charge distributions formed in various MNT reactions is shown in Fig. 5 for the following reactions:  $^{58}\text{Ni} + ^{208}\text{Pb}$  at  $E_{\text{c.m.}} = 270$  MeV [56],  $^{64}\text{Ni} + ^{208}\text{Pb}$  at  $E_{\text{c.m.}} = 268$  MeV [57],  $^{136}\text{Xe} + ^{208}\text{Pb}$  at  $E_{\text{c.m.}} = 526$  MeV [58],  $^{136}\text{Xe} + ^{208}\text{Pb}$  at  $E_{\text{c.m.}} = 617$  MeV [58], and  $^{208}\text{Pb} + ^{208}\text{Pb}$  at  $E_{\text{c.m.}} = 786$  MeV [59]. One can see from each panel of Fig. 5 that the calculated distributions of the production cross sections are reasonably consistent with experimental results.

*Summary.* In this Letter, we have developed the DNS-sysu model aimed at providing a comprehensive and unified description of QE, DI, and QF channels in MNT reactions. The improved DNS-sysu model presented here incorporates a multidimensional master-equation-based diffusion approach, which allows for a realistic simulation of the stochastic nucleon exchange process during

the interaction of two heavy nuclei. The validity and predictive power of the model were benchmarked against a broad set of experimental data, covering reactions such as  $^{40}\text{Ca}$ ,  $^{58,64}\text{Ni}$ ,  $^{136}\text{Xe}$ , and  $^{208}\text{Pb} + ^{208}\text{Pb}$ . The calculated isotopic, mass, and charge distributions of the reaction products exhibit strong consistency with the experimental measurements. One of the key improvements of the DNS model in this work is the inclusion of partial impact-parameter-dependent transition probabilities, which enhances the description of both grazing collisions and DIC. This unified approach is particularly valuable for identifying optimal reaction systems and beam energies to access unexplored regions of the nuclear chart.

Nevertheless, there remain open challenges and opportunities for future development. One possible direction is the integration of microscopic inputs, such as single-particle energy levels and nucleon density distributions from constrained density functional theory, to provide more accurate potential energy surfaces and transition rates.

*Acknowledgments.* The authors would like to thank Pei-Wei Wen and Gen Zhang for helpful discussion and suggestions. This work was supported by the National Natural Science Foundation of China under Grants No. 12075327 and 12475136.

- 
- [1] G. Adamian, N. Antonenko, A. Diaz-Torres, and S. Heinz, How to extend the chart of nuclides?, *The European Physical Journal A* **56**, 1 (2020).
  - [2] R. Broda, Spectroscopic studies with the use of deep-inelastic heavy-ion reactions, *Journal of Physics G: Nu-*

- clear and Particle Physics **32**, R151 (2006).
- [3] Y. Hirayama and K. Collaboration, Progress of isotope separators and kiss facility for the study of exotic nuclei, *The European Physical Journal Special Topics* **233**, 1209 (2024).

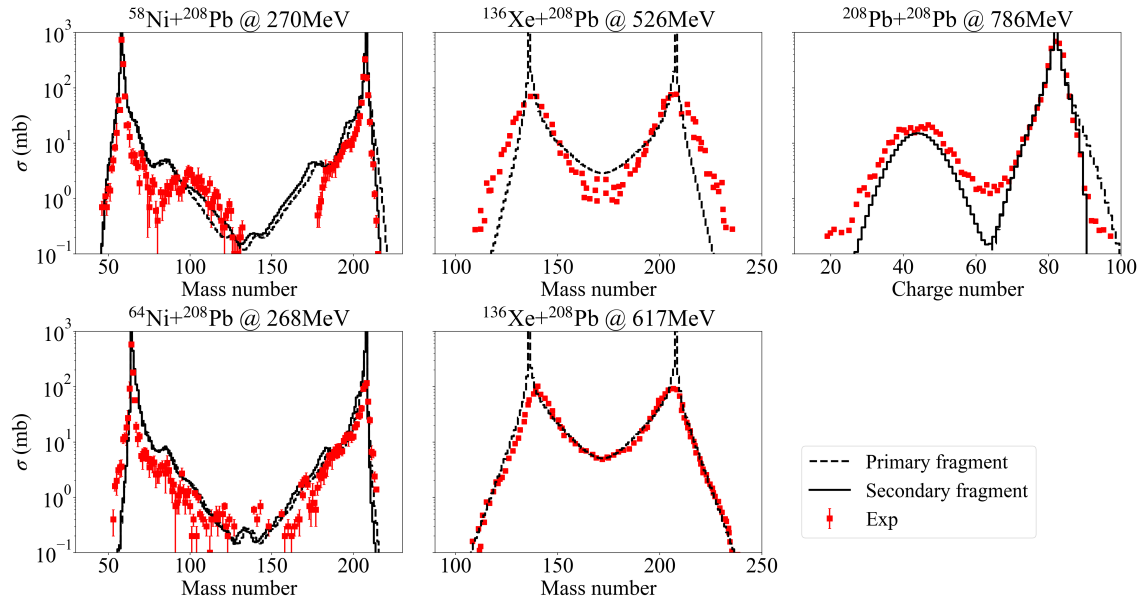


FIG. 5. Mass or charge distributions for reaction products. The measured cross sections are shown by red squares with error bars, which were taken from Refs [56–59]. Black dotted line represents the results of the improved DNS-sysu calculations, while the black solid line represents the results of the improved DNS-sysu + GEMINI++ calculations.

- [4] L. Corradi, G. Pollarolo, and S. Szilner, Multinucleon transfer processes in heavy-ion reactions, *Journal of Physics G: Nuclear and Particle Physics* **36**, 113101 (2009).
- [5] R. Pérez-Vidal, F. Galtarossa, T. Mijatović, S. Szilner, I. Zanon, D. Brugnara, J. Pellumaj, M. Ciemala, J. J. Valiente-Dobón, L. Corradi, *et al.*, Nuclear structure advancements with multi-nucleon transfer reactions, *The European Physical Journal A* **59**, 114 (2023).
- [6] D. Hinde, M. Dasgupta, and E. Simpson, Experimental studies of the competition between fusion and quasifission in the formation of heavy and superheavy nuclei, *Progress in Particle and Nuclear Physics* **118**, 103856 (2021).
- [7] E. M. Kozulin, G. N. Knyazheva, T. K. Ghosh, A. Sen, I. M. Itkis, M. G. Itkis, K. V. Novikov, I. N. Diatlov, I. V. Pchelintsev, C. Bhattacharya, S. Bhattacharya, K. Banerjee, E. O. Saveleva, and I. V. Vorobiev, Fission and quasifission of the composite system  $z = 114$  formed in heavy-ion reactions at energies near the coulomb barrier, *Phys. Rev. C* **99**, 014616 (2019).
- [8] E. M. Kozulin, G. N. Knyazheva, K. V. Novikov, I. M. Itkis, M. G. Itkis, S. N. Dmitriev, Y. T. Oganessian, A. A. Bogachev, N. I. Kozulina, I. Harca, W. H. Trzaska, and T. K. Ghosh, Fission and quasifission of composite systems with  $z = 108 - 120$ : Transition from heavy-ion reactions involving s and ca to ti and ni ions, *Phys. Rev. C* **94**, 054613 (2016).
- [9] C. Li, J. Tian, and F.-S. Zhang, Production mechanism of the neutron-rich nuclei in multinucleon transfer reactions: A reaction time scale analysis in energy dissipation process, *Physics Letters B* **809**, 135697 (2020).
- [10] H. Yao, C. Li, H. Zhou, and N. Wang, Distinguishing fission-like events from deep-inelastic collisions, *Phys. Rev. C* **109**, 034608 (2024).
- [11] A. Winther, Grazing reactions in collisions between heavy nuclei, *Nuclear Physics A* **572**, 191 (1994).
- [12] A. Winther, Dissipation, polarization and fluctuation in grazing heavy-ion collisions and the boundary to the chaotic regime, *Nuclear Physics A* **594**, 203 (1995).
- [13] G. G. Adamian, N. V. Antonenko, and W. Scheid, Characteristics of quasifission products within the dinuclear system model, *Phys. Rev. C* **68**, 034601 (2003).
- [14] A. Nasirov, A. Fukushima, Y. Toyoshima, Y. Aritomo, A. Muminov, S. Kalandarov, and R. Utamuratov, The role of orientation of nucleus symmetry axis in fusion dynamics, *Nuclear Physics A* **759**, 342 (2005).
- [15] Z.-Q. Feng, G.-M. Jin, and J.-Q. Li, Production of heavy isotopes in transfer reactions by collisions of  $^{238}\text{U} + ^{238}\text{U}$ , *Phys. Rev. C* **80**, 067601 (2009).
- [16] W. Li, N. Wang, J. F. Li, H. Xu, W. Zuo, E. Zhao, J. Q. Li, and W. Scheid, Fusion probability in heavy-ion collisions by a dinuclear-system model, *Europhys. Lett.* **64**, 750 (2003).
- [17] X. J. Bao, Role of neutron excess in the projectile for the production of heavy neutron-rich nuclei, *Phys. Rev. C* **102**, 054613 (2020).
- [18] P. W. Wen, A. K. Nasirov, C. J. Lin, and H. M. Jia, Multinucleon transfer reaction from view point of dynamical dinuclear system method, *Journal of Physics G: Nuclear and Particle Physics* **47**, 075106 (2020).
- [19] A. V. Karpov and V. V. Saiko, Modeling near-barrier collisions of heavy ions based on a langevin-type approach, *Phys. Rev. C* **96**, 024618 (2017).
- [20] V. Zagrebaev and W. Greiner, Unified consideration of deep inelastic, quasi-fission and fusion-fission phenomena, *Journal of Physics G: Nuclear and Particle Physics* **31**, 825 (2005).
- [21] F. C. Dai, P. W. Wen, C. J. Lin, J. J. Liu, X. X. Xu, K. L. Wang, H. M. Jia, L. Yang, N. R. Ma, and F. Yang, Theoretical study of multinucleon transfer reactions by coupling the langevin dynamics iteratively with the mas-



- ter equation, Phys. Rev. C **109**, 024617 (2024).
- [22] L. Zhu, New model based on coupling the master and langevin equations in the study of multinucleon transfer reactions, Physics Letters B **849**, 138423 (2024).
- [23] Y. Yang *et al.*, Production of actinide isotopes near  $\theta_{\text{lab}}=0^\circ$  in multinucleon transfer reaction  $^{238}\text{U} + ^{248}\text{Cm}$ , Phys. Lett. B **862**, 139318 (2025).
- [24] K. Zhao, Z. Liu, F. Zhang, and N. Wang, Production of neutron-rich  $n=126$  nuclei in multinucleon transfer reactions: Comparison between  $^{136}\text{Xe} + ^{198}\text{Pt}$  and  $^{238}\text{U} + ^{198}\text{Pt}$  reactions, Physics Letters B **815**, 136101 (2021).
- [25] C. Li, P. Wen, J. Li, G. Zhang, B. Li, X. Xu, Z. Liu, S. Zhu, and F.-S. Zhang, Production mechanism of new neutron-rich heavy nuclei in the  $\text{Xe}^{136} + ^{198}\text{Pt}$  reaction, Physics Letters B **776**, 278 (2018).
- [26] K. Sekizawa and K. Yabana, Time-dependent hartree-fock calculations for multinucleon transfer processes in  $^{40,48}\text{Ca} + ^{124}\text{Sn}$ ,  $^{40}\text{Ca} + ^{208}\text{Pb}$ , and  $^{58}\text{Ni} + ^{208}\text{Pb}$  reactions, Phys. Rev. C **88**, 014614 (2013).
- [27] D. D. Zhang, D. Vretenar, T. Nikšić, P. W. Zhao, and J. Meng, Multinucleon transfer with time-dependent covariant density functional theory, Phys. Rev. C **109**, 024614 (2024).
- [28] A. S. Umar, C. Simenel, and W. Ye, Transport properties of isospin asymmetric nuclear matter using the time-dependent hartree-fock method, Phys. Rev. C **96**, 024625 (2017).
- [29] L. Guo, C. Shen, C. Yu, and Z. Wu, Isotopic trends of quasifission and fusion-fission in the reactions  $^{48}\text{Ca} + ^{239,244}\text{Pu}$ , Phys. Rev. C **98**, 064609 (2018).
- [30] S. Ayik, M. Arik, E. Erbayri, O. Yilmaz, and A. S. Umar, Multinucleon transfer mechanism in  $^{160}\text{Gd} + ^{186}\text{W}$  collisions in stochastic mean-field theory, Phys. Rev. C **108**, 054605 (2023).
- [31] Z. Gao, K. Sekizawa, and L. Zhu, Time-dependent random phase approximation for particle-number fluctuations and correlations in deep-inelastic collisions of  $^{144}\text{Sm} + ^{144}\text{Sm}$  and  $^{154}\text{Sm} + ^{154}\text{Sm}$ , Phys. Rev. C **112**, 014602 (2025).
- [32] V. V. Volkov, Deep inelastic transfer reactions—the new type of reactions between complex nuclei, Physics Reports **44**, 93 (1978).
- [33] J. Li, G. Zhang, X. Zhang, Y. Zhang, Z. Liu, and F.-S. Zhang, Production of unknown neutron-rich transuranium isotopes 245–249np, 248–251pu, 248–254am, and 252–254cm in multinucleon transfer reactions, Journal of Physics G: Nuclear and Particle Physics **49**, 025106 (2022).
- [34] G. Zhang and F.-S. Zhang, Production of neutron-rich nuclei near  $N=126$  in multinucleon transfer reactions with potential pockets, Phys. Rev. C **111**, 014603 (2025).
- [35] X.-K. Le, F.-Z. Xing, S.-Q. Guo, and N. Wang, Theoretical study of the angular distribution of reaction products from the  $^{136}\text{Xe} + ^{208}\text{Pb}$  and  $^{238}\text{U} + ^{248}\text{Cm}$  reactions, Phys. Rev. C **111**, 024618 (2025).
- [36] Z. Liao, Z. Gao, Y. Yang, L. Zhu, and J. Su, Shell effects on the drift and fluctuation in multinucleon transfer reactions, Phys. Rev. C **109**, 054612 (2024).
- [37] P.-w. Wen, C. Li, L. Zhu, C.-j. Lin, and F.-s. Zhang, Mechanism of multinucleon transfer reaction based on the grazing model and dns model, Journal of Physics G: Nuclear and Particle Physics **44**, 115101 (2017).
- [38] L. Zhu and J. Su, Unified description of fusion and multinucleon transfer processes within the dinuclear system model, Phys. Rev. C **104**, 044606 (2021).
- [39] V. Saiko and A. Karpov, Multinucleon transfer as a method for production of new heavy neutron-enriched isotopes of transuranium elements, The European Physical Journal A **58**, 41 (2022).
- [40] G. Wolschin and W. Nörenberg, Analysis of relaxation phenomena in heavy-ion collisions, Zeitschrift für Physik A Atoms and Nuclei **284**, 209 (1978).
- [41] L. Zhu, P.-W. Wen, C.-J. Lin, X.-J. Bao, J. Su, C. Li, and C.-C. Guo, Shell effects in a multinucleon transfer process, Physical Review C **97**, 044614 (2018).
- [42] V. Zagrebaev and W. Greiner, Shell effects in damped collisions: a new way to superheavies, Journal of Physics G: Nuclear and Particle Physics **34**, 2265 (2007).
- [43] W. D. Myers and W. J. Swiatecki, Nuclear masses and deformations, Nuclear Physics **81**, 1 (1966).
- [44] C. Y. Wong, Interaction barrier in charged-particle nuclear reactions, Phys. Rev. Lett. **31**, 766 (1973).
- [45] G. Adamian, N. Antonenko, R. Jolos, S. Ivanova, and O. Melnikova, Effective nucleus-nucleus potential for calculation of potential energy of a dinuclear system, International Journal of Modern Physics E **5**, 191 (1996).
- [46] Q. Li, W. Zuo, W. Li, N. Wang, E. Zhao, J. Li, and W. Scheid, Deformation and orientation effects in the driving potential of the dinuclear model, The European Physical Journal A-Hadrons and Nuclei **24**, 223 (2005).
- [47] G. Haag, Modelling with the master equation (2017).
- [48] L. Moretto and J. Sventek, A theoretical approach to the problem of partial equilibration in heavy ion reactions, Physics Letters B **58**, 26 (1975).
- [49] V. Zagrebaev and W. Greiner, Cross sections for the production of superheavy nuclei, Nuclear Physics A **944**, 257 (2015).
- [50] V. Zagrebaev, Sub-barrier fusion enhancement due to neutron transfer, Physical Review C **67**, 061601 (2003).
- [51] W. Von Oertzen, H. Bohlen, B. Gebauer, R. Küinkel, F. Pühlhofer, and D. Schüllh, Quasi-elastic neutron transfer and pairing effects in the interaction of heavy nuclei, Zeitschrift für Physik A Atomic Nuclei **326**, 463 (1987).
- [52] L. Corradi, A. M. Vinodkumar, A. M. Stefanini, E. Fioretto, G. Prete, S. Beghini, G. Montagnoli, F. Scarlassara, G. Pollarolo, F. Cerutti, and A. Winther, Light and heavy transfer products in  $^{58}\text{Ni} + ^{208}\text{Pb}$  at the coulomb barrier, Phys. Rev. C **66**, 024606 (2002).
- [53] R. J. Charity, Systematic description of evaporation spectra for light and heavy compound nuclei, Phys. Rev. C **82**, 014610 (2010).
- [54] T. Mijatović, S. Szilner, L. Corradi, D. Montanari, G. Pollarolo, E. Fioretto, A. Gadea, A. Goasduff, D. J. a. c. Malenica, N. Mărginean, M. Milin, G. Montagnoli, F. Scarlassara, N. Soić, A. M. Stefanini, C. A. Ur, and J. J. Valiente-Dobón, Multinucleon transfer reactions in the  $^{40}\text{Ar} + ^{208}\text{Pb}$  system, Phys. Rev. C **94**, 064616 (2016).
- [55] S. Szilner, L. Corradi, G. Pollarolo, S. Beghini, B. R. Behera, E. Fioretto, A. Gadea, F. Haas, A. Latina, G. Montagnoli, F. Scarlassara, A. M. Stefanini, M. Trotta, A. M. Vinodkumar, and Y. Wu, Multinucleon transfer processes in  $^{40}\text{Ca} + ^{208}\text{Pb}$ , Phys. Rev. C **71**, 044610 (2005).
- [56] W. Królas, R. Broda, B. Fornal, T. Pawlat, J. Wrzesiński, D. Bazzacco, G. de Angelis, S. Lunardi, R. Menegazzo, D. Napoli, and C. Rossi Alvarez, Dynamical deformation of nuclei in deep-inelastic collisions: A gamma co-incidence study of  $^{130}\text{Te} + 275\text{ MeV } ^{64}\text{Ni}$  and  $^{208}\text{Pb} + 345\text{ MeV } ^{58}\text{Ni}$  heavy ion reactions, Nuclear Physics A **832**,

- 170 (2010).
- [57] W. Królas, R. Broda, B. Fornal, T. Pawlat, H. Grawe, K. Maier, M. Schramm, and R. Schubart, Gamma coincidence study of  $^{208}\text{Pb} + 350 \text{ MeV } ^{64}\text{Ni}$  collisions, *Nuclear Physics A* **724**, 289 (2003).
  - [58] E. M. Kozulin, E. Vardaci, G. N. Knyazheva, A. A. Bogachev, S. N. Dmitriev, I. M. Itkis, M. G. Itkis, A. G. Knyazev, T. A. Loktev, K. V. Novikov, E. A. Razinkov, O. V. Rudakov, S. V. Smirnov, W. Trzaska, and V. I. Zagrebaev, Mass distributions of the system  $^{136}\text{Xe} + ^{208}\text{Pb}$  at laboratory energies around the coulomb barrier: A candidate reaction for the production of neutron-rich nuclei at  $N = 126$ , *Phys. Rev. C* **86**, 044611 (2012).
  - [59] T. Tanabe, R. Bock, M. Dakowski, A. Gobbi, H. Sann, H. Stelzer, U. Lynen, A. Olmi, and D. Pelte, The  $\text{pb} + \text{pb}$  collision, *Nuclear Physics A* **342**, 194 (1980).